Optimization for the HP-CORD UV chemical decontamination process for AISI 304 stainless steel

Nuclear Engineering and Design 414 (2023) 112550

Contents lists available at ScienceDirect

Nuclear Engineering and Design

journal homepage: www.elsevier.com/locate/nucengdes

Optimization for the HP-CORD UV chemical decontamination process for AISI 304 stainless steel

Marino Corrado [a,b], Silvio Cao [b], Sabrina Grassini [c], Leonardo Iannucci [c], Laura Savoldi [a,*]

[a] Dipartimento Energia "Galileo Ferraris", Politecnico di Torino, Torino I-10129, Italy
[b] Green-land S.R.L., Via Aldo Moro 5, Brescia I-25100, Italy
[c] Dipartimento Scienza Applicata e Tecnologia, Politecnico di Torino, Torino I-10129, Italy

A B S T R A C T

The decontamination of stainless-steel surfaces in Light Water Reactors components, that may suffer from nuclear activation and contamination, is still a topic that deserves research and development studies. In this paper, the HP-CORD-UV chemical method for the removal of thin surface layers from AISI 304 stainless steel samples is addressed, considering multiple cycles of oxidation and cleaning. A procedure for the optimization of the oxidation phase considering in particular the pH of the solution, the ($[KMnO_4]/[H^+]$ ratio), and the immersion time (oxidation time), was developed and is here presented. The experimental results show that 10 oxidation cycles at pH 3, $[MnO_4^-] = [H^+]$, for 2 h, followed by 30 min of cleaning in oxalic acid, allowed to reach a thickness of dissolved metal of about 3–4 μm. Despite the intrinsic localised morphology of the corrosion attack on AISI 304 sample surface, scanning electron microscopy showed good reproducibility of the process.

1. Introduction

As part of the decommissioning of nuclear reactors, one of the major problems is the nuclear activation and contamination of many components of the reactor (Pretzsch et al., 2012) (pipes, tanks, equipment, etc.). At the end of the plant lifetime such components become low- or medium-activity waste, and they must be properly disposed. As a matter of fact, in the primary circuits of a LWRs the surface layer of the stainless-steel typically dissolves in water, gets close to the core, gets irradiated, becomes activated, and then re-deposits in the primary circuit. In particular, Iron has impurities of Co-59 which become Co-60 (gamma emitter) after neutron irradiation. Moreover, if some micro leaks of the fuel take place (as it can occur during 40 years of operation), some fission products and actinides diffuse out in the water and deposit on the superficial layer of the primary circuit.

The high-level safety requirements and the amount of such wastes make the decommissioning procedures time and money-consuming (MacKerron, 1989). Since most of the contaminated surfaces of a nuclear power plant are localized in the primary circuits (Juodis et al., 2019), in the latest decades technological research has addressed metallic surface decontamination (Zhong et al., 2021), focusing mainly on inox and carbon steel (Pujol Pozo et al., 2019). Recent studies (NEA Task Group on Decontamination, 1998) suggest that chemical decontamination methods for non-activated metallic inner components of the Light Water Reactors (LWRs), with activity below 1 Bq/g, are the most efficient and promising procedures to recycle the decontaminated material in conventional metallurgical plants, reducing the amount of low- and medium-activity waste. Chemical methods owe their success to the possibility to work remotely and to regenerate the used chemicals. One of the performance indicators of the decontamination process is the Decontamination Factor (DF), defined as the ratio between the contamination level of the material before decontamination and the contamination level after decontamination (Sun et al., 2019).

It is nowadays well established (Yang et al., 1996; Pick and Segal, 1983) that the composition of the contaminated inner layer of the primary circuit highly depends on the history of the nuclear reactor (material composition, operation and decommissioning time, possible fuel rods breaks, water chemistry of the primary circuits, operation temperature and pressure). In LWRs, both pressurized (PWRs) and boiling water (BWRs) reactors, the surface contamination is confined in a micrometer layer constituted mainly by iron, chromium, and nickel oxides in which radioactive impurities deposit. Analysing chemical decontamination processes, the study in (Speranzini et al., 1987) addressed the effect of the oxalic acid concentration on the base metal corrosion rate, focusing on AISI 304 and AISI 410 stainless steels. Note that ideally the AISI 304 should not be corroded, but after 40 years in a high

* Corresponding author.
E-mail addresses: marino.corrado@polito.it, marino.corrado@green-land.it (M. Corrado), caosilvio@tiscali.it (S. Cao), sabrina.grassini@polito.it (S. Grassini), leonardo.iannucci@polito.it (L. Iannucci), laura.savoldi@polito.it (L. Savoldi).

https://doi.org/10.1016/j.nucengdes.2023.112550
Received 2 May 2023; Received in revised form 16 July 2023; Accepted 14 August 2023
Available online 21 August 2023

temperature and pressure environment, a corrosion layer might form. In this case, iron and nickel oxide can be removed by oxalic acid. The chromium oxide, instead, turns out to be too stable and cannot be removed by oxalic acid. Moreover, drawbacks were investigated, such as the corrosion effects induced unintentionally on the base metal when strong chemical decontamination methods are adopted (Kass et al., 1984).

Different chemical decontamination processes have been tested based on low- or high-chemicals, i.e. using solutions with a concentration below or above 0.2%, respectively (Zhong et al., 2021; NEA Task Group on Decontamination, 1998). Low-chemicals methods exhibit the advantage of producing a reduced volume of chemical waste and of consuming a limited amount of Ion EXchange resins (IEXs) for the final water radiological cleaning. However, they have significantly lower performance (DF < 5) compared to high-chemicals methods (DF up to 100). On the other side, in the recent past high-chemicals methods have acquired greater reliability thanks to the improvements in regenerative chemical techniques, which make them economically and ecologically more sustainable. Actually, modern techniques are based on the use of a concentrated solution of a reducing agent (such as oxalic and citric acid) capable of dissolving the contaminated layer. After this step, all the radioactive ions are properly removed by the IEXs. The ion solubility in the water is ensured, enhanced, and controlled by pH regulation and by adding complexing agents such as EDTA (Ethilene Diamine Tetraacetic Acid), NTA (Nitrilo Triacetic Acid) and HEDTA (Hydroxy Ethylethylen Diamine Triacetic Acid), which complex iron, nickel, chromium ions increasing their solubility (Keny et al., 2005). It is worth noting that the environment for surface decontamination is typically harsh; a study by Keny et al. (Keny et al., 2005) addressed the efficiency of the complexing agents under gamma radiation exposure.

When the decontamination is to be performed on stainless steel surfaces, the reducing agent loses its efficiency due to the presence of a stable superficial layer of chromium oxides which covers the underlying layers of the contaminated surface (Ohmi et al., 1996). In this case, a single-step treatment turns out to be ineffective and, before the reduction step, an oxidizing solution must be used first, to oxidize the Cr^{+3} of the oxide layer in a more soluble Cr^{+6} and to dissolve it (Ohmi et al., 1996). Many two-step methods exist depending on the oxidizing agent, the reducing agent, and on the complexing agent such as APAC (Alkaline Permanganate followed by Ammonium Citrate), APACE (APAC with additional EDTA as complexing agent), APOX (Alkaline Permanganate followed by OXalic acid), AP-CITOX (Alkaline Permanganate followed by CITric and OXalic acid) (Chen et al., 1997). The efficiency in terms of DF for each of these products depends on the type of stainless steel (thus on its chemical composition), on the concentration of reagents, on the time and temperature of the process. In case of efficiency below the target value, several decontamination cycles should be performed in series, until satisfying results are achieved. Many processes use the permanganate anion (MnO_4^-) as oxidising agent because of its excellent efficacy. The oxidation effectiveness of MnO_4^- is affected by solution pH and it is higher in acid environment, as demonstrated in (Tian et al., 2019).

The HP-CORD-UV is a two-step chemical decontamination process designed for the treatment of inox and carbon steel (Ketusky, 2017). In the first step (the **oxidizing** phase) the acid solution of permanganate attacks the metallic surface dissolving part of the superficial oxide layer. Note that the oxidation phase is essential in the process to oxidize the Cr^{+3} to Cr^{+6}: if chromium was not treated, the stable Cr oxide layer would make the cleaning phase ineffective. In the second step (**cleaning** phase) a concentrated solution of oxalic acid with some percentage of EDTA dissolves the oxide layer and reduces the remaining permanganate. Generally, from two to three cycles are carried out before reaching a satisfying DF value (i.e. DF > 100). All the radioactive ions are then captured by IEXs. At the end of the oxidizing-cleaning cycles, as most of the ions dissolved in the solution come from the contaminated layer, all other ions are properly neutralized to avoid an extensive and unnecessary use of IEXs. Finally, the excess of oxalic acid is chemically decomposed to H_2O and O_2 by oxidation from a concentrated solution of H_2O_2 under ultra-violet light. As explained, the HP-CORD process minimizes the use of IEXs for radioactive capture and in theory does not produce chemical waste. This makes it one of the most promising processes for the decontamination of LWRs.

As a matter of fact, the effectiveness of two-step chemical decontamination processes depends on the total DF that they reach, on the ability to attack uniformly the surface of interest, on the amount of the chemical and radioactive waste produced (Chen et al., 1997). All the chemical reactions taking place in the dissolution of iron oxide in acid solution are described extensively in (Panias et al., 1996). Since the chemistry involved in these reactions is well-known, the research is now focusing on the optimization of the process. In this work, addressing specifically the HP-CORD-UV (Tian et al., 2019) process, a procedure to optimize the main parameter of the whole process is identified. More specifically, in this work the number of oxidizing-reducing cycles is experimentally investigated on pristine (i.e., non-activated) samples of AISI 304 stainless steel, to find the optimal value, optimizing the minimal operation time, the reagents concentration, and the uniformity of the acid attack. The choice of the type of stainless steel is driven by the target application, i.e. the decommissioning of the Enrico Fermi electrical Nuclear Power plant in Italy, the primary circuit of which is mainly made in AISI 304 rather than the most commonly used AISI 316/L. The oxidation phase in the tests is performed using a solution of nitric acid (HNO_3) and potassium permanganate ($KMnO_4$), while the reducing phase is performed by means of a highly concentrated solution of oxalic acid. Suspension of the radioactive ions in the water matrix and their capture in the IEXs are instead beyond the scope of this paper.

2. Methodology

In this section, the experimental set-up (including the employed materials and instrumentation) is illustrated, together with the sampling techniques adopted for the analysis of the specimens.

2.1. Sample preparation

The investigation was carried out on pristine (i.e. non-activated) AISI 304 stainless steel samples, characterised by the chemical composition reported in Table 1. Each specimen had the dimensions of 30 mm $\times$ 30 mm $\times$ 5 mm. No surface treatment was performed on the samples prior to use.

To carry out the immersion tests mimicking the decontamination process, different solutions were prepared. The oxidation step was performed using different solutions of potassium permanganate ($KMnO_4$, purchased from "Fine Chemicals") in distilled water. The pH of the solutions was adjusted using nitric acid (HNO_3, purchased from "Panreac"). The cleaning step was performed using a solution of oxalic acid ($C_2H_2O_4$, purchased from "Materia Madre") in distilled water. The concentration of the oxalic acid solution was kept constant in all experiments and was equal to 8 wt% (Wiersma et al., 2007), and the pH was not modified.

The immersion tests were carried out placing the stainless-steel samples in beakers containing a fixed volume of solution equal to 250 ml (one specimen per beaker). All immersion tests were performed at the temperature of 80 °C, both during the oxidation step in potassium permanganate and during the cleaning step in oxalic acid. The volume of solution was kept constant in all tests to avoid possible variability in the

Table 1
Composition of the AISI304 samples.

Composition (wt%)			
C	**Cr**	**Ni**	**Fe**
<0.07%	17.5%-19.5%	8.0%-10%	balance

results due to the ratio between the volume of solution and the surface area of the sample. When longer immersion times were performed (i.e., in tests lasting more than two hours) in the oxidation phase, the solution was replaced by a new one every two hours of immersion, to eliminate the possible effect related to the presence of a limiting reagent (in this case permanganate), which would slow down the reaction after a certain immersion time.

After the immersion tests, the cross-section of some samples was analysed by electron microscopy. To perform this characterisation, the samples were encapsulated in cold embedding resin (Technovit 4071) and then sectioned by a metallographic cutting machine. The cross-sections were polished using abrasive papers with increasingly finer grains from 800 to 2500 grit and then cloths. Final polishing was carried out using diamond paste up to 1-μm size. Before analyzing the samples with the electron microscope, they were coated by a 10-nm layer of platinum, to make their surface conductive. The deposition of the platinum layer was performed by direct current sputtering, using the QT150S Quorum Sputter Coater instrument with the following deposition conditions: pressure of 5×10^{-3} mbar, current of 60 μA, and duration of 20 s.

Field Emission Scanning Electron Microscope (FESEM Zeiss Supra40) with an acceleration voltage of 5 kV and a numerical aperture of 30 μm was used to perform the SEM analyses.

2.2. Optimization procedure for the oxidation solution

The optimization procedure adopted in this work is summarized in Fig. 1. As reported in previous studies (Pujol Pozo et al., 2019), four parameters have a major influence on the process:

- pH of the solution,
- the ratio between the molar concentration of potassium permanganate and H^+ ions ($[KMnO_4]/[H^+]$),
- the immersion time in the solution during the oxidation phase (oxidation time),
- the temperature of the solution.

As the temperature affects the reactions kinetics, to simplify the problem it was not changed in the different tests, and it was set to 80 °C. The process can be considered optimized when the user reaches a balance between the oxide layer homogeneity and its thickness. Actually, when working with stainless steels, the corrosive attack has always a localised morphology, and a more aggressive environment leads to lower homogeneity in the final result.

In the first step of the optimization procedure, the pH and oxidation time were varied to obtain a homogeneous oxide layer grown on the sample. In this step, the molar concentration of potassium permanganate [$KMnO_4$] was set equal to the concentration of H^+ (related to the solution pH). The effectiveness of the oxidation step was investigated by visual inspection only.

In the second step of the optimization procedure, the $[KMnO_4]/[H^+]$ ratio should be adjusted to maximize the oxide thickness after immersion. Results were first investigated by visual inspection and then by SEM analysis to measure the thickness of the oxide layer.

Using this optimization procedure, it was possible to screen rapidly many operative conditions for the oxidation step, checking the results only by a simple visual inspection. Actually, a non-homogeneous result should be discarded regardless of the obtained oxide layer thickness, and this can be easily assessed without specific instrumentation. In the second step, the thickness of the oxide layer was measured only for the promising test conditions, as the analysis by SEM is more expensive and time-consuming.

3. Experimental results

3.1. Effect of pH and oxidation time on corrosion attack

A set of AISI304 samples were immersed in solutions of different aggressiveness, to evaluate the effect of pH, and for different oxidation times to also evaluate the effect of the process duration. The tested pH values were equal to 3, 4, and 5. All tests have been carried out at a temperature of about 80 °C, for a total duration of 2 h, 4 h, or 6 h. The test matrix is summarized in Fig. 2. In all cases, the concentration of permanganate ions [MnO_4^-] is equal to those of hydrogen ions [H^+] (pH related). As discussed previously, the effect of permanganate ions was evaluated in the subsequent set of samples.

The first step of the procedure aimed at evaluating the attack morphology and its homogeneity, so the extension and depth of the corrosive attack on the surface were qualitatively estimated by visual inspection, to estimate the effect of pH and oxidation time on the oxidation kinetics. Fig. 2 shows that the corrosive attack on stainless steel coupons occurs preferentially on some areas of the sample surface. The location of the corrosive attack differs from sample to sample, depending on the material microscopic surface defects and

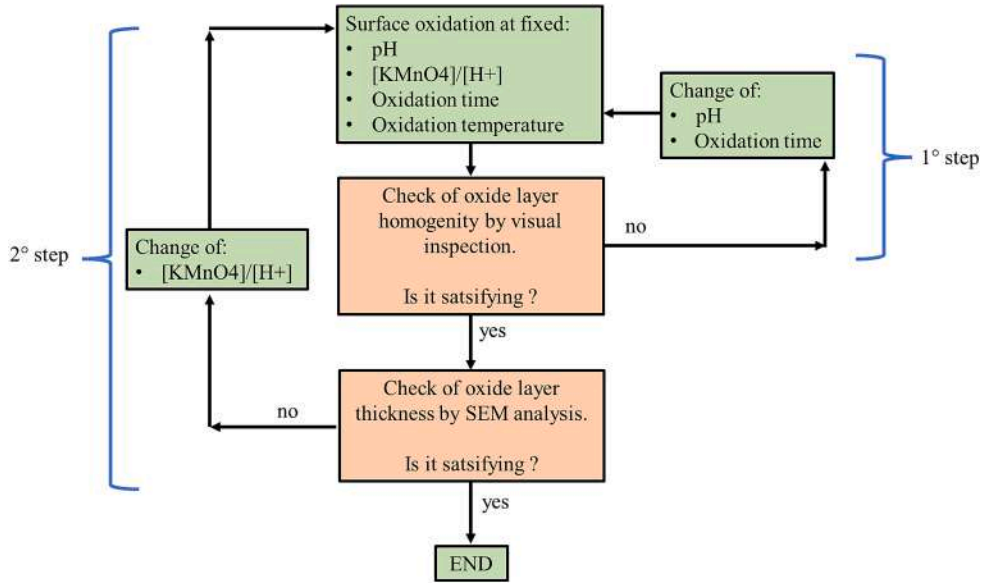

Fig. 1. Flowchart of the optimization procedure adopted in this research.

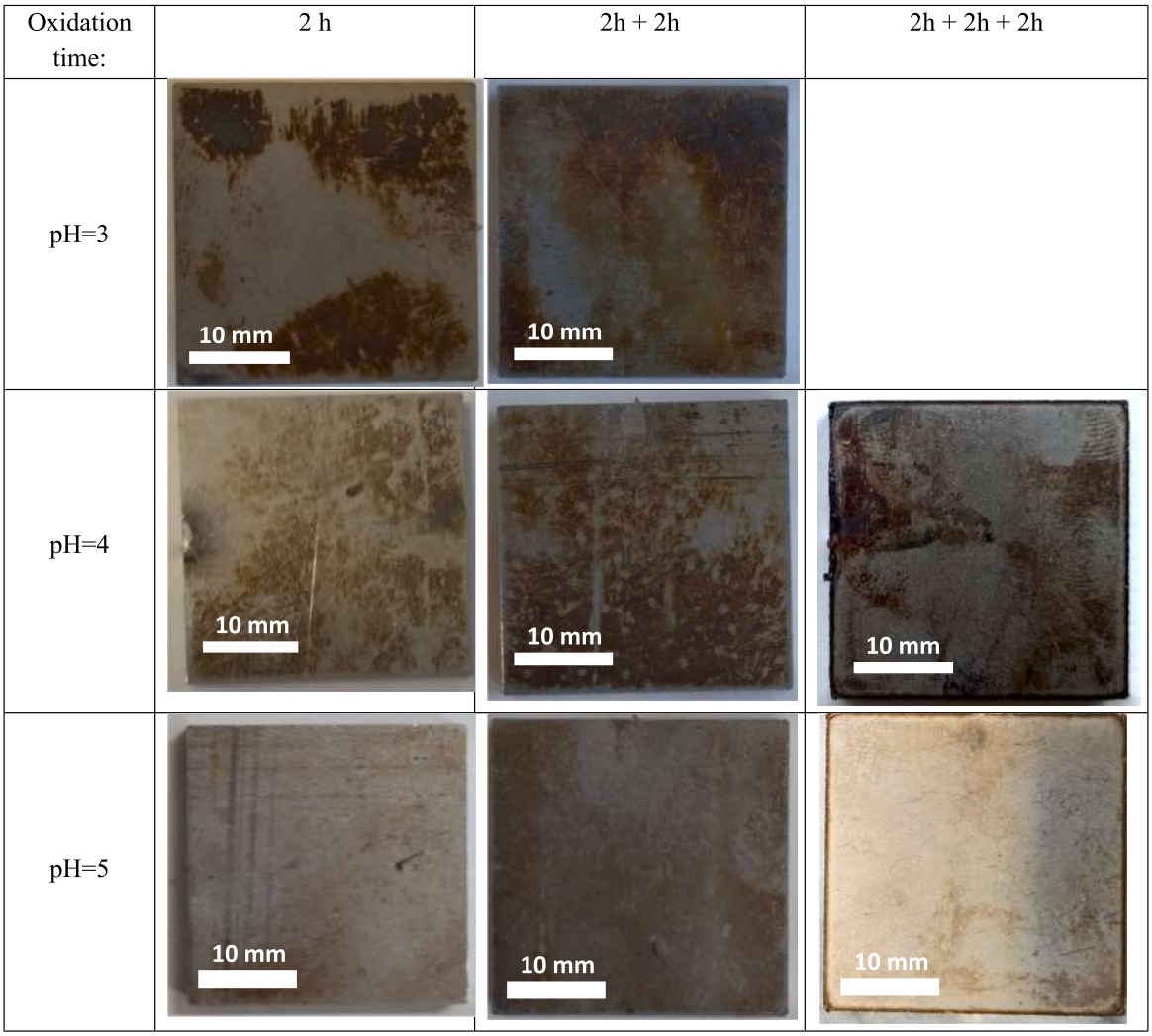

Fig. 2. Picture of the sample surfaces as they result from the first set of immersion tests, $[MnO_4^-] = [H^+]$ for all tests.

heterogeneity. In fact, in this class of steels, the corrosive attack always proceeds in a preferential way starting from defects or discontinuities present on the surface of the material (at the macroscopic or even just microscopic scale). Moreover, results show that at low pH (pH = 3) the corrosive attack is more localized, and the oxide layer appears to be thicker by visual inspection. At higher pH (pH = 5), the thickness of the oxide layer is thinner but more uniform.

It is also verified that in the most aggressive solution (i.e. at low pH), with longer immersion time the thickness of the oxide layer increases, but unfortunately the attack morphology is more inhomogeneous. In fact, as expected for this material, oxidation continues preferentially over time in areas already previously attacked and not in those still intact. This is a clear limit for the application of this process, as it does not allow removing a uniform layer of material from the specimen. To obtain a more uniform attack morphology, a less aggressive solution and longer operating times are needed.

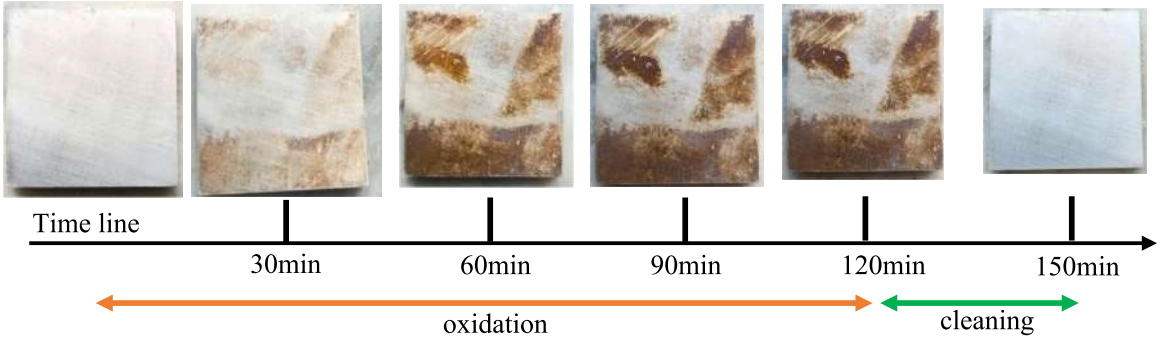

Fig. 3. Photographs of samples at increasing values of immersion time in potassium permanganate solution (30 min, 60 min, 90 min, 120 min) and after 30 min of oxalic acid immersion. Each sample is 30 × 30 × 5 mm^3.

3.2. Oxidation and cleaning time optimization

To optimize the overall duration of the process, the morphology of the attack was visually assessed after 30-minute intervals. A permanganate solution with pH = 3 and $[H^+]/[MnO4^-] = 1$ was used in the oxidation phase while a 8 wt% oxalic acid solution was used in the cleaning phase. The effect of the oxidizing solution after 30 min, 60 min, 90 min, and 120 min and the effect of cleaning after 30 min are shown in Fig. 3.

The sample oxidation clearly continues throughout the 120-minute immersion process. Actually, small but visible differences are present between the sample immersed for 90 and for 120 min in the potassium permanganate solution. On the contrary, oxalic acid cleans effectively already after only 30 min. According to these results, oxidation and cleaning times were set to 2 h and 30 min respectively, to reduce the overall process time.

3.3. Effect of permanganate concentration on corrosion attack

After evaluating the effect of pH and oxidation time, the solutions with pH = 4 and 5 were taken into consideration to analyze the effects of a higher permanganate concentration. The aim was to obtain a faster kinetics of oxidation of the metal using a more aggressive solution, still keeping the attack as uniform as possible. Fig. 4 shows the test conditions investigated and the results in this second set of experiments. The samples were immersed for 4 h.

The obtained results show, at first visual inspection, different behaviours for the samples immersed in solution with pH = 4 and pH = 5. In fact, in the first case (Fig. 4(a) and (b)) the attack took place preferentially in a specific area of the sample (closer to the edges), leaving almost unchanged the central part. On the contrary, in the sample immersed in solution at pH equal to 5 (Fig. 4(c)), the morphology of the attack was more uniform, although the oxide thickness, by a preliminary visual inspection, appeared lower. It is possible to observe that the higher concentration of permanganate allowed to accelerate the kinetics of oxidation, without over-emphasising the localized character of the attack.

Before immersion in the oxidising solution, untreated steel samples have an oxide thickness of a few nanometers. This is the oxide layer that spontaneously grows on stainless steels surface in contact with air. Considering its thickness, it cannot be observed by electron microscopy, but more sophisticated analyses should be carried out, such as XPS (X-Ray Photoelectron Spectroscopy) (Detriche et al., 2020).

After immersion in the permanganate solution, the thickness of the oxide layer increases and thus it can be detected by SEM observation. Analysing the cross-section of the samples by backscattered electrons detector, the oxide layer can be identified as the interface region between the metal and the embedding resin. Indeed, the oxide layer appears as a light-grey region, because this area has a different chemical composition; actually, using the backscattered electrons detector, the material appears lighter when its atomic weight is higher.

To assess quantitatively the thickness of the oxide layer, two samples were then prepared for SEM observation:

- a sample immersed for 4 h in a solution with pH = 5 and permanganate ion concentration of 10^{-5} mol/l,
- a sample immersed for 4 h in a solution with pH = 5 and permanganate ion concentration equal to 6×10^{-5} mol/l.

The results for the two samples are reported in Fig. 5 and Fig. 6, respectively. In the former, the oxide thickness is ranging from 0.3 μm and 1 μm. These values agree with the visual inspection of the sample, in which the oxide layer appears rather thin (see Fig. 2).

For the second sample, the increase in the oxide thickness was much more evident and values between 1 μm and 1.7 μm have been measured, as reported in Fig. 6.

3.4. Oxalic acid effectiveness in the cleaning phase

As a final set of experiments, the behaviour of the material in different complete oxidation-cleaning cycles was evaluated. Each cycle consists of two hours of immersion in a solution of potassium permanganate solution (oxidation phase) followed by a 30 mins immersion in an oxalic acid solution (cleaning phase, concentration of 8 wt%).

Two were the oxidizing solutions assessed in this phase: the one at pH = 5 and $[MnO_4^-] = 6 \times [H^+]$ and the one at pH = 3 and $[MnO_4^-] = [H^+]$. They were chosen to be representative of two different conditions: the former for a uniform attack (the permanganate concentration was increased to accelerate the kinetics) and the second for a more severe but inhomogeneous oxidation.

Actually, the effectiveness of the oxalic acid solution in the cleaning phase influences also the choice of the most appropriate solution in the oxidation phase. If cleaning is found to be not very effective, the oxidizing solution must be as weak as possible, in order to avoid a localized attack that would be accentuated in subsequent cycles. On the contrary, a very effective cleaning would allow using a more aggressive solution in the oxidation phase, because the effects of the localized attack would be largely eliminated during the cleaning phase and therefore the subsequent oxidation would always proceed in a localized way, but in different areas. Therefore, the optimal aggressiveness of the oxidizing solution depends on the cleaning effectiveness of the oxalic acid. In the present study, for this set of experiments it was decided to polish the surface of the samples using coarse-grained sanding papers (400 grit), to reduce the variability of the results due to the different initial surface finish in the various samples (presence of defects, surface inhomogeneities etc.). After polishing, the surface conditions are similar

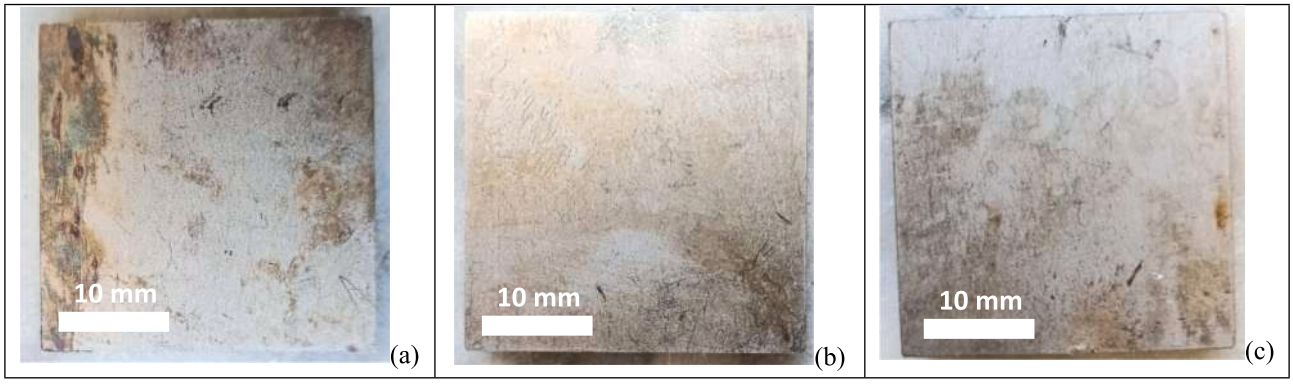

Fig. 4. Results of the second set of immersion tests: sample immersed for 4 h in the solution with concentration $[MnO_4^-] = 3 \times [H^+]$ and with pH = 4 (a) or pH = 5 (b), and in the solution with concentration $[MnO_4^-] = 6 \times [H^+]$ and with pH = 5 (c).

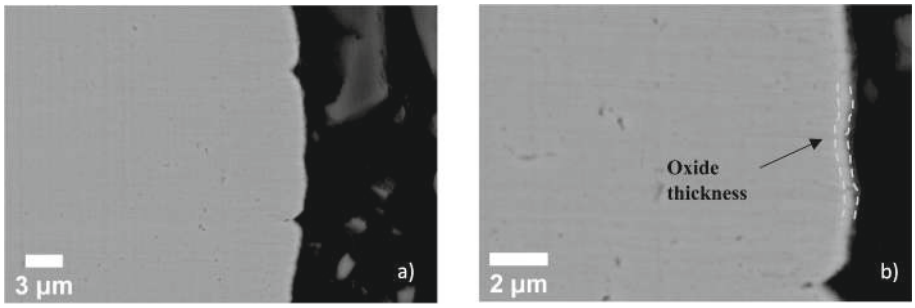

Fig. 5. Two SEM images (a & b) of the sample immersed for four hours in a pH 5 solution with ion concentration permanganate equal to 10^{-5} mol/l. Both images were acquired using the Backscattered Electrons detector.

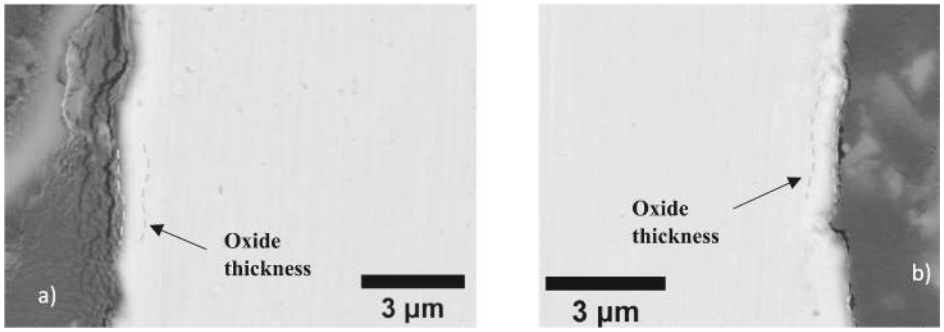

Fig. 6. Two SEM images of the left (a) and right (b) borders of the sample immersed for four hours in a pH 5 solution with a permanganate ion concentration of $6{\cdot}10^{-5}$ mol/l. On micrograph, the oxide layer is highlighted. Both images were acquired using the Backscattered Electrons detector.

for all samples and thus results are expected to be more reproducible. Results are shown in Fig. 7 and Fig. 8, and they clearly show the great effectiveness of the cleaning step, which is able to completely remove the oxide layer grown during the immersion in the permanganate solution.

Fig. 9 and Fig. 10 show the appearance of the samples surface after each immersion in the two solution. It is possible to observe that the corrosive attack takes place in different areas of the sample at each cycle. In the cleaning phase, the oxalic acid is able to dissolve the oxide previously formed and it eliminates the major macroscopic defects of the surface. Therefore, the subsequent oxidation takes place in different areas. This proves the excellent cleaning effect of the oxalic acid and explains the reason why the successive oxidations appear in different areas in each cycle. In addition, experiments (Fig. 10) have shown that after the oxidation phase, the oxide growth seems to reduce in the cycles following the first one.

Since the pH 5 solution was found to be very weak (Fig. 9), it was decided to use the more effective solution with pH = 3 in the last part of this study. Although the attack at pH = 3 is strongly localized (Fig. 10), the excellent cleaning made by the oxalic acid guarantees the sample surface to return to a finish similar to the initial one. For this reason, the subsequent oxidation during the following cycles (all done with the same duration of the oxidation and cleaning phases) could proceed randomly in a localized manner, but (statistically) in other areas of the sample. Oxide layer will progressively grow on all areas of the sample after an appropriate number of cycles.

3.5. Assessment of the removed steel thickness after 10 cycles (oxidation + cleaning)

After selecting the most effective solutions for the oxidation-cleaning treatment and optimizing the immersion times, the last test evaluated the thickness of material removed during the oxidation and cleaning process. Part of the sample was embedded in resin to protect it from the oxidation and cleaning treatments, as sketched in Fig. 11. Two samples have been tested: first they were subjected to 10 cycles (oxidation and cleaning) and then they were analyzed by SEM.

The measurements showed that a thickness of about 3 to 4 µm was removed during the process (Fig. 12). It is worth to notice that the result is not perfectly uniform for all samples and some parts of the cross-

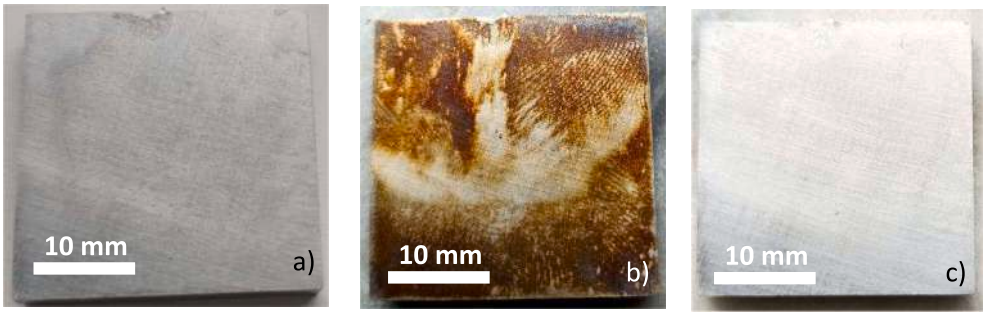

Fig. 7. A) initial sample. b) sample after oxidation in ph 3 solution ($[MnO_4\text{-}] = [H^+]$). c) sample after one oxidation-cleaning cycle (permanganate oxidation + oxalic acid cleaning).

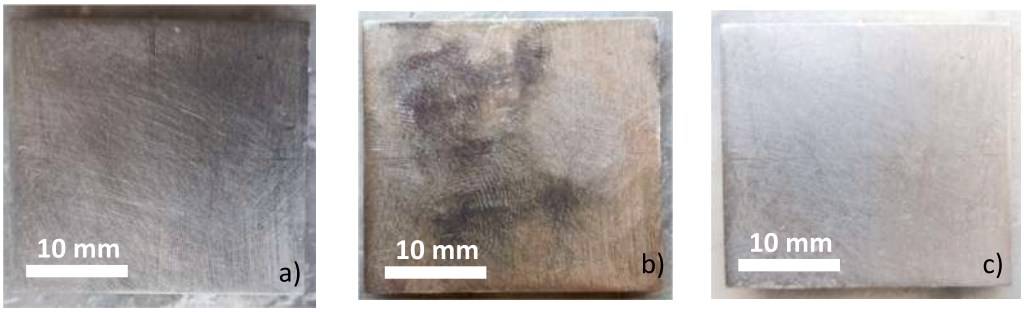

Fig. 8. A) initial sample. b) sample after oxidation in ph 5 solution ([MnO_4-] = 6[H^+]). c) sample after one oxidation-cleaning *cycle* (permanganate oxidation + oxalic acid cleaning).

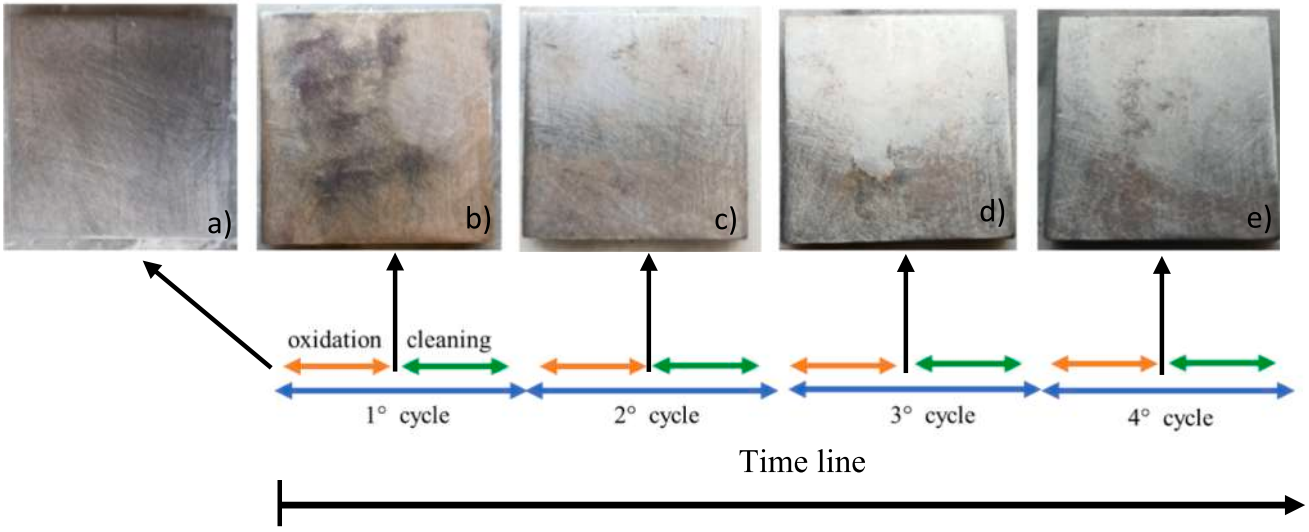

Fig. 9. Sample at initial condition (a) and after each of the four immersion cycles in permanganate solution at pH 5 (b, c, d, e). Sample dimension is 30 × 30 × 5 mm^3.

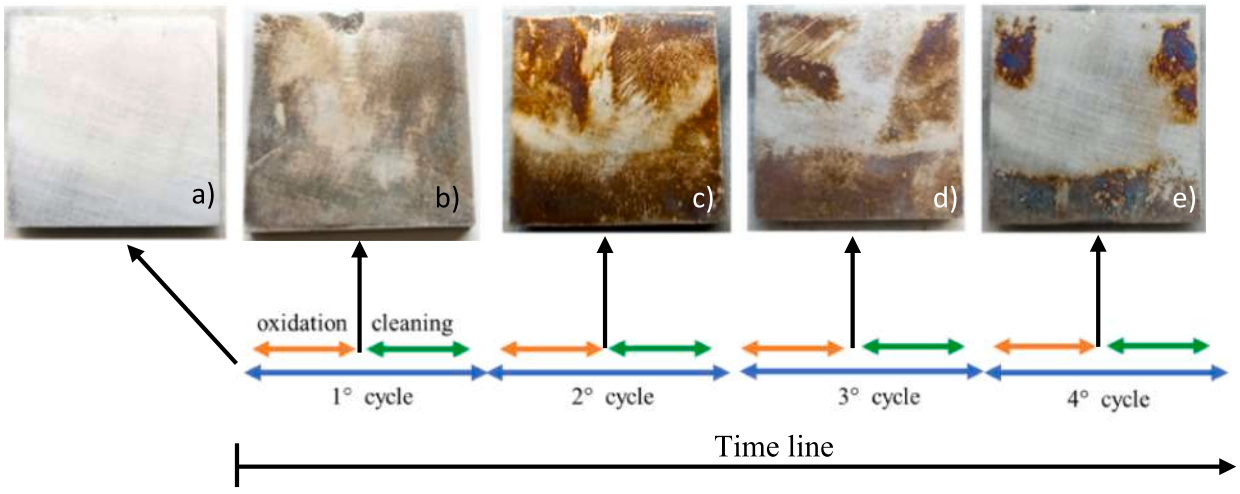

Fig. 10. Sample at initial condition (a) and after each of the four immersion cycles in permanganate solution at pH 3 (b, c, d, e). Sample dimension is 30 × 30 × 5 mm^3.

section exhibit higher depth of attack respect to others.

Thus, this analysis confirms the effectiveness of the multiple cycles of oxidation and cleaning, but at the same time it underlines the importance of performing a sufficient number of cycles in order to remove enough material from the steel surface.

4. Conclusion and future perspectives

The chemical dissolution of a superficial layer of AISI304 by means of HP Cord process has been experimentally reproduced and demonstrated. Considering the excellent results obtained in the cleaning phase

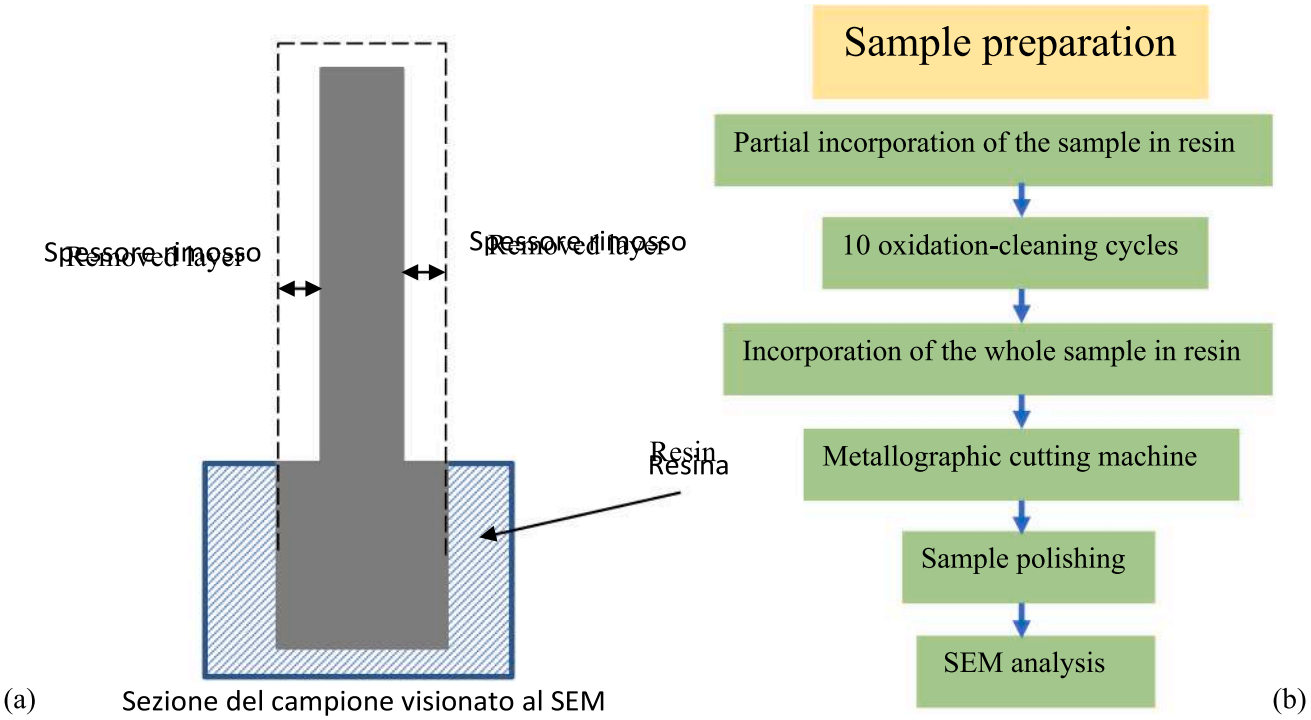

Fig. 11. (a) Representation of the sample produced to measure the thickness of material removed after 10 cycles of oxidation and cleaning. (b) Procedure for the sample preparation.

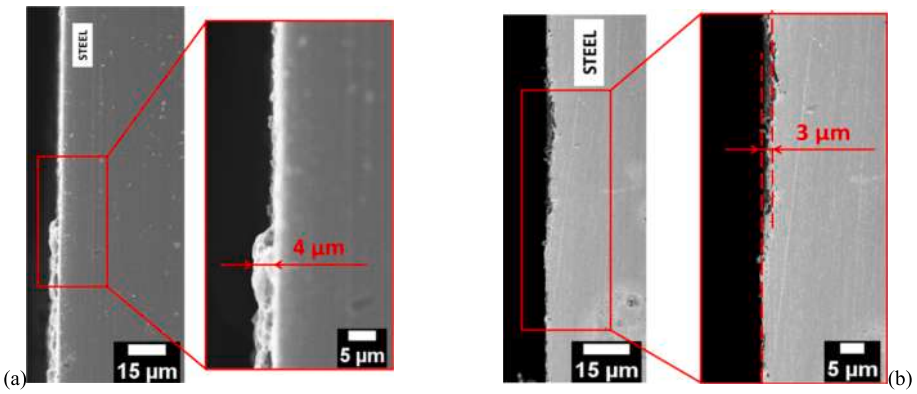

Fig. 12. SEM images of two specimens (a)&(b) showing the thickness of the metal layer removed by 10 oxidation-cleaning cycles. Images acquired using the Secondary Electrons detector.

in oxalic acid, it was found that the best oxidizing solution for the oxidation phase is the most aggressive one among those studied (pH = 3 and potassium permanganate concentration equal to 10^{-3} M). This choice accelerates the dissolution of the metal reducing the number of cycles required. The optimal immersion time in the permanganate solution (oxidation step) has been found to be 2 h, with a duration of the cleaning step of 30 min. Note that the duration of the cleaning step may be further optimized and reduced below 30 min.

The oxidation kinetics of the metal in the permanganate solution were evaluated by visual observations and electron microscopy. The results showed a clear dependence of the dissolution process on the pH and the immersion time. Since the solution with pH = 3 has a very marked oxidizing effect on the surface of the sample, an immersion time of two hours has been retained. For the solutions with a higher pH, better results were obtained by increasing the permanganate concentration or immersion time.

Considering the results obtained in the tests, the best-performing oxidizing solution was found to be the one with pH = 3 and $[MnO_4]$ = $[H^+]$. As a final analysis, the thickness of dissolved metal after 10 cycles (oxidation and cleaning) was measured using electron microscopy. Despite the intrinsic localised corrosion attack of stainless steel, the process succeeded in removing a homogeneous layer of about 3–4 µm from the AISI304 sample surface.

In this study, a 8 %wt. oxalic acid solution was used in the cleaning cycle, but a solution containing a lower concentration of oxalic acid will be evaluated in the future to reduce the reagents amount in the process. Moreover, to prevent the chemicals from acting as limiting reagents during the oxidation and cleaning process, the needed volume of the solutions in the present study was probably over-estimated. An optimisation of the solution volume, according to the area of material to be decontaminated, might contribute to decrease the amount of chemicals and final chemical waste volume.

CRediT authorship contribution statement

Marino Corrado: Conceptualization, Methodology, Validation,

Formal analysis, Investigation, Data curation, Writing – original draft, Visualization. **Silvio Cao:** Conceptualization, Supervision. **Sabrina Grassini:** Conceptualization, Methodology, Writing – review & editing. **Leonardo Iannucci:** Conceptualization, Methodology, Validation, Formal analysis, Investigation, Writing – original draft, Visualization. **Laura Savoldi:** Writing – review & editing, Supervision, Funding acquisition.

Declaration of Competing Interest

The authors declare that they have no known competing financial interests or personal relationships that could have appeared to influence the work reported in this paper.

Data availability

Data will be made available on request.

References

Chen L, Chamberlain DB, Conner C, Vandegrift GF. 1997. A Survey of Decontamination Processes Applicable to DOE Nuclear Facilities.

Detriche, S., Vivegnis, S., Vanhumbeeck, J.-F., Felten, A., Louette, P., Renner, F.U., Delhalle, J., Mekhalif, Z., 2020. XPS fast depth profile of the native oxide layers on AISI 304, 316 and 430 commercial stainless steels and their evolution with time. J. Electron. Spectros. Relat. Phenomena 243, 146970.

Juodis, L., Maceika, E., Plukis, A., Dacquait, F., Genin, J.-B., Benier, G., 2019. Assessment of radioactive contamination in primary circuit of WWER-440 type reactors by computer code OSCAR for the decommissioning case. Progr. Nucl. Energy 110, 191–198. https://doi.org/10.1016/j.pnucene.2018.09.019.

Kass JN, Wang MT, Clarke WL, Odegaard TK, Walker WL, Gordon BM. 1984. Corrosion implications for chemical decontamination and preservice treatment for BWRs. ANS Executive Conference on Decontamination of Power Reactors, Springfield, Mass.

Keny, S.J., Kumbhar, A.G., Venkateswaran, G., Kishore, K., 2005. Radiation effects on the dissolution kinetics of magnetite and hematite in EDTA- and NTA-based dilute chemical decontamination formulations. Radiat. Phys. Chem. 72, 475–482. https://doi.org/10.1016/j.radphyschem.2003.12.055.

Ketusky E. 2017. Remediation of Spent Oxalic Acid Nuclear Decontamination Solutions using Ozone.

MacKerron, G., 1989. The decommissioning of nuclear plant: Timing, cost and regulation. Energy Policy 17, 103–108. https://doi.org/10.1016/0301-4215(89)90088-8.

NEA Task Group on Decontamination. Decontamination Techniques Used in Decommissioning Activities, 1998.

Ohmi T, Nakagawa Y, Nakamura M, Ohki A, Koyama T. 1996. Formation of chromium oxide on 316L austenitic stainless steel. J. Vacuum Sci. Technol. A.14:2505–10. Doi: 10.1116/1.580010.

Panias, D., Taxiarchou, M., Paspaliaris, I., Kontopoulos, A., 1996. Mechanisms of dissolution of iron oxides in aqueous oxalic acid solutions. Hydrometallurgy 42 (2), 257–265.

Pick, M.E., Segal, M.G., 1983. Chemical decontamination of water reactors. CEGB developments and the international scene. Nucl. Energy 22, 433–444.

Pretzsch G, Gmal B, Hesse U, Hummelsheim K. Neutron. 2012, activation of reactor components during operation lifetime of a NPP. Nuclear Power Plant Life Management Proceedings of An International Symposium, Int. Atomic Energy Agency (IAEA), pp. 1CD-ROM.

Pujol Pozo, A.A., Bustos Bustos, E., Monroy-Guzmán, F., 2019. Decontamination of radioactive metal surfaces by electrocoagulation. J. Hazard. Mater. 361, 357–366. https://doi.org/10.1016/j.jhazmat.2018.08.061.

Speranzini, R.A., Tapping, R.L., Disney, D.J., 1987. Corrosiveness of Decontamination Solutions to Sensitized AISI 304 Stainless Steel. Corrosion 43, 632–641. https://doi.org/10.5006/1.3583842.

Sun, H., Sibamoto, Y., Okagaki, Y., Yonomoto, T., 2019. Experimental Investigation of Decontamination Factor Dependence on Aerosol Concentration in Pool Scrubbing. Sci. Technol. Nucl. Installat. 2019, 1743982. https://doi.org/10.1155/2019/1743982.

Tian, Z., Song, L., Li, X., 2019. Effect of Oxidizing Decontamination Process on Corrosion Property of 304L Stainless Steel. Int. J. Corrosion 2019, 1–6.

Wiersma, B, John Mickalonis, J, Michael Poirier, M, John Pareizs, J, David Herman, D, David Beam, D, Samuel Fink, S, and Fernando Fondeur, F. 2007. "IN-SITU MONITORING OF CORROSION DURING A LABORATORY SIMULATION OF OXALIC ACID CHEMICAL CLEANING". United States. https://www.osti.gov/servlets/purl/918136.

Yang, I.J., Teng, M.Y., Huan, W.I., Sun, Y.L., 1996. Decontamination of the reactor coolant pump in Maanshan nuclear power plant. Nucl. Eng. Design 167, 91–97. https://doi.org/10.1016/S0029-5493(96)01247-2.

Zhong, L., Lei, J., Deng, J., Lei, Z., Lei, L., Xu, X., 2021. Existing and potential decontamination methods for radioactively contaminated metals-A Review. Progr. Nucl. Energy 139, 103854. https://doi.org/10.1016/j.pnucene.2021.103854.